THE ASTROPHYSICAL JOURNAL, 545:449–453, 2000 December 10

IN-FLIGHT CALIBRATION OF THE *ROSAT* HRI ULTRAVIOLET SENSITIVITY

M. BARBERA,[1] G. MICELA,[1] A. COLLURA,[2] S. S. MURRAY,[3] AND M. V. ZOMBECK[3]

Received 2000 February 15; accepted 2000 July 25

ABSTRACT

Comparing measured and estimated count rates of a few selected sample stars, we confirm the validity and provide the in-flight calibration of the *ROSAT* HRI UV/visible effective area model in Zombeck et al. The count rate estimates for Betelgeuse derived with this model are in agreement with the measured HRI upper limit. This result is also confirmed in an erratum by Berghöfer et al. aimed at revising their previous calculation, which was overestimated by more than 2 orders of magnitude. Adopting this *ROSAT* HRI UV/visible effective area model and measured UV/visible spectra of a set of sample stars covering the range of $T_{\rm eff}$ 3000–40,000 K, we have built the calibration curves to estimate UV/visible contamination count rates for any star of known $T_{\rm eff}$, m_v, and $N_{\rm H}$.

Subject headings: instrumentation: detectors — stars: early-type — stars: late-type — ultraviolet: stars — X-rays: stars

1. INTRODUCTION

The unexpected UV sensitivity of the *ROSAT* HRI (David et al. 1995) has been a compelling issue, both for the interpretation of the HRI data of sources with a potential UV component and for the design and calibration of the HRC on board the *Chandra X-Ray Observatory* (Murray et al. 1997), a multichannel plate detector similar to the *ROSAT* and *Einstein* HRIs.

The paper by Zombeck et al. (1997, hereafter Paper I) has provided experimental evidence that the excess *ROSAT* HRI UV sensitivity is due to a higher than originally expected transmission of the UV/Ion blocking filters. At least two effects are responsible for this higher transmission: oxidation of the aluminum layers and resonant interference introduced by their multilayer design (Barbera et al. 1997). As a result, a significant contribution to the HRI UV sensitivity occurs at wavelengths longer than 2000 Å in agreement with pulse-height distributions observed for hot stars indicating UV detections at wavelengths longer than 1850 Å (in-flight calibration line).

The HRI UV quantum efficiency model given in Figure 4 of Paper I is based on laboratory measurements of backup filters and microchannel plates. It shows that, besides the sensitivity at wavelengths longer than 2000 Å, a contribution to the UV sensitivity is still present in the 1200–2000 Å band previously ascribed as the only source of UV leak in the *Einstein* HRI (Schmitt et al. 1985). Given the inadequate knowledge of the UV/visible sensitivity of CsI-coated microchannel plates, the HRI effective-area model presented in Paper I provides two different curves for wavelengths longer than 2500 Å. These are representative of the lower and upper limits for the actual HRI UV sensitivity.

Berghöfer, Schmitt, & Hünsch (1999) claimed that the effective-area model presented in Paper I overestimates the HRI quantum efficiency at wavelengths longer than 2500 Å and support this argument on the basis of a comparison between the measured upper limit to the HRI count rate for Betelgeuse and the count rate they estimated using that model. More recently, stimulated by our further investigations on the subject, these authors have recalculated the Betelgeuse-estimated HRI count rate and found a new estimate about 2 orders of magnitude lower and in agreement with the validity of the model in Paper I (Berghöfer, Schmitt, & Hünsch 2000).

In order to verify the accuracy of the UV/visible effective-area model presented in Paper I and to provide an in-flight calibration of the model, we have analyzed a set of sample stars of different spectral types observed with both the *ROSAT* PSPC and HRI. The UV/visible spectra of these sample stars, which have been folded with the HRI effective-area model to estimate the expected UV/visible contamination, are based on *International Ultraviolet Explorer* (*IUE*) observations (1200–3250 Å) of the sample stars and normalized, optical, calibrated spectra of parent spectral-type stars (3500–7400 Å).

Once the HRI UV/visible effective-area model, based on laboratory measurements (Paper I), is validated and calibrated with the use of *ROSAT* HRI in-flight measurements, we can use this model to estimate the expected UV/visible count rate contamination for stellar observations conducted with the *ROSAT* HRI.

In § 2 we compare the measured HRI count rates for a set of sample stars with the estimated count rates based on our effective-area model provided in Paper I. In § 3 we show for which spectral-type stars it is important to account for possible HRI UV/visible contamination and provide the curves to estimate the HRI count rates due to UV/visible contamination for any star of given photospheric effective temperature ($T_{\rm eff}$), apparent visual magnitude (m_v), and interstellar hydrogen column density ($N_{\rm H}$).

2. IN-FLIGHT CALIBRATION OF THE HRI UV/VISIBLE EFFECTIVE-AREA MODEL

In order to provide the in-flight calibration of the HRI UV/visible effective-area model presented in Paper I, we have selected a set of sample stars observed with both the *ROSAT* PSPC and the HRI detectors, where an *IUE*-calibrated, low-dispersion spectrum was available. Beside a few early-type stars where the UV/visible contamination can be significant, we have also included, for completeness, a few late-type stars.

[1] Osservatorio Astronomico, G.S. Vaiana, Palermo, Italy; barbera@oapa.astropa.unipa.it.
[2] Istituto per le Applicazioni Interdisciplinari della Fisica (CNR), Palermo, Italy.
[3] Harvard-Smithsonian Center for Astrophysics, Cambridge, MA.

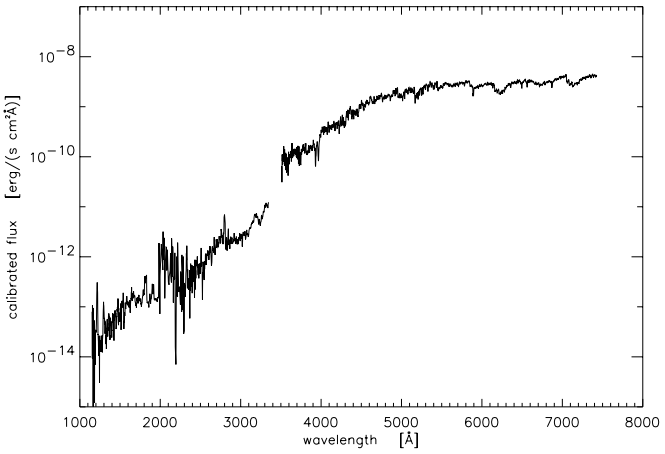

FIG. 1.—UV/visible calibrated spectrum of Betelgeuse

Table 1 lists the selected sample stars including the measured *ROSAT* PSPC and HRI count rates. To estimate the HRI UV/visible contamination count rates, we have used measured, calibrated spectra. The UV spectra of the sample stars in the wavelength range 1200–3250 Å are based on calibrated low-dispersion spectra taken with the *IUE* and available in the public archive maintained by the European Space Agency at VILSPA.[4] The visible spectra 3500–7400 Å have been derived from calibrated spectra of parent spectral-type stars in Jacoby, Hunter, & Christian (1984). The gap between 3250 and 3500 Å has been filled with a linear interpolation between the UV and the visible spectra. Table 1 lists the ID numbers of the specific *IUE* observations used for each sample star. As an example, Figure 1 shows the calibrated UV/visible spectrum of Betelgeuse.

Table 2 reports the estimated count rates in different wavelength ranges derived using the HRI effective-area model published in Paper I. The last column gives the measured *ROSAT* HRI UV/visible contamination count rate. Notice that for the stars with negligible X-ray emission, inferred from the *ROSAT* PSPC measurement, the measured *ROSAT* HRI UV/visible contamination count rate coincides with the measured HRI rate (see Table 1). For the other stars, the measured PSPC rate has been converted into the expected X-ray HRI rate using the PIMMS software with a single-temperature Raymond-Smith (RS) model. This rate was then subtracted from the measured HRI rate to derive the residual UV/visible contamination rate. The parameters used in the RS model are, namely, HD 46150 ($kT = 0.86$ keV, $N_H = 2.2 \times 10^{21}$), ζ Orionis ($kT = 0.22$ keV, $N_H = 3.0 \times 10^{20}$), γ Cassiopeia ($kT = 0.86$ keV, $N_H = 2.0 \times 10^{20}$), Alcyone ($kT = 0.86$ keV, $N_H = 2.0 \times 10^{20}$), Hz 2168 ($kT = 0.86$ keV, $N_H = 2.0 \times 10^{20}$), GJ 124 ($kT = 0.86$ keV, $N_H = 1.0 \times 10^{18}$), and GJ 139 ($kT = 0.86$ keV, $N_H = 1.0 \times 10^{18}$). The $\log(N_H)$ is available in the literature for all these stars. The temperature has been taken from Berghöfer, Schmitt, & Cassinelli (1996) for ζ Orionis, and γ Cassiopeia, while for the other stars we have used a typical value of $kT = 0.86$ keV. The uncertainty in the plasma temperature should not introduce a relative uncertainty larger than 20% in the estimated PSPC-to-HRI rate conversion factor.

For all of our sample stars, the estimated *ROSAT* HRI count rates, resulting from the leak in the 1200–5500 Å band, are consistent with the measured total count rates.

The estimated count rates suggest that a nonnegligible contribution to the HRI UV sensitivity comes at wavelengths longer than 2500 Å. As discussed in Paper I, the poor knowledge of the microchannel plate quantum efficiency at wavelengths longer than 2500 Å results in a somewhat uncertain knowledge of the HRI effective area at these wavelengths. The two models, provided in Paper I, above 2500 Å define the range where the actual HRI effective area should be located. The comparison between estimated and measured count rates for early-type stars and, in particular, the detections suggest that the actual HRI effective area is likely to be closer to the high effective-area model provided in Paper I.

In the case of the late-type star Betelgeuse, the UV contamination is only at wavelengths longer than 2000 Å with a nonnegligible contribution in the wavelength range 4000–5500 Å. The *ROSAT* HRI upper limit to the count rate from Betelgeuse is consistent with both the effective-

[4] http://iuearc.vilspa.esa.es/.

TABLE 1

LIST OF ADOPTED SAMPLE STARS WITH BOTH PSPC AND HRI OBSERVATIONS

Star	HR	HD	Spectral Type	V	PSPC Rate	HRI Rate	*IUE* Spectra
		46150	O6e	6.75	0.056 ± 0.002[a]	0.018 ± 0.001[a]	SWP 08325, LWR 07268
ζ Ori.....	1948	37742	O9 Iab	1.70	1.45 ± 0.01[a]	0.700 ± 0.005[a]	SWP 33048, LWP 11671
γ Cas	264	5394	B0 IVe	2.39	3.79 ± 0.03[a]	1.336 ± 0.008[a]	SWP 33893, LWP 13607
Alcyone	1165	23630	B7 III	2.87	<0.003[b]	0.0138 ± 0.0008[c]	SWP 08020, LWR 07078
Hz 2168	1178	23850	B8 III	3.62	<0.006[b]	0.0072 ± 0.0015[c]	SWP 11245, LWR 09867
Rigel.....	1713	34085	B8 Iab	0.12	<0.0015[d]	0.1960 ± 0.0096[d]	SWP 31880, LWP 11654
Vega	7001	172167	A0 V	0.03	<0.001[d]	0.0937 ± 0.0035[d]	SWP 27024, LWP 07904
β Aur.....	2088	40183	A2 IV	1.85	<0.002[d]	0.0078 ± 0.0019[d]	SWP 50172, LWP 27602
β Car	3685	80007	A2 IV	1.70	<0.0004[d]	0.0111 ± 0.0010[d]	SWP 43459, LWP 22059
GJ 124	937	19373	G0 V	4.05	0.055 ± 0.002[e]	0.011 ± 0.002[a]	SWP 02663, LWR 02376
GJ 139	1008	20794	G8 V	4.27	0.0070 ± 0.0005[e]	0.0029 ± 0.0009[a]	SWP 14039, LWR 12242
Betelgeuse.....	2061	39801	M1	0.50	<0.012[d]	<0.0005[d]	SWP 37517, LWP 19982

[a] Archival data processed by SASS.
[b] Archival data processed by the wavelet detection algorithm in Damiani et al. 1997.
[c] Micela et al. 1996.
[d] Micela et al. 1999.
[e] Berghöfer et al. 1999.

TABLE 2

ESTIMATED AND MEASURED HRI UV/VISIBLE CONTAMINATION COUNT RATES

STAR	ESTIMATED RATES[a]					MEASURED RATE
	1200–2000 Å	2000–2500 Å	2500–4000 Å	4000–5500 Å	1200–5500 Å	
HD 46150.....	2×10^{-4}	2×10^{-4}	2×10^{-5}, 2×10^{-4}	3×10^{-8}, 2×10^{-6}	3×10^{-4}, 5×10^{-4}	$< 5 \times 10^{-3}$[b]
ζ Ori.....	4×10^{-2}	7×10^{-2}	9×10^{-3}, 6×10^{-2}	5×10^{-6}, 3×10^{-4}	1×10^{-1}, 2×10^{-1}	3×10^{-1}[b]
γ Cas	3×10^{-2}	4×10^{-2}	4×10^{-3}, 3×10^{-2}	3×10^{-6}, 2×10^{-4}	7×10^{-2}, 9×10^{-2}	$< 3 \times 10^{-1}$[b]
Alcyone	3×10^{-3}	5×10^{-3}	6×10^{-4}, 5×10^{-3}	1×10^{-6}, 8×10^{-5}	9×10^{-3}, 1×10^{-2}	0.014 ± 0.002[b]
Hz 2168	2×10^{-3}	2×10^{-3}	3×10^{-4}, 2×10^{-3}	7×10^{-7}, 4×10^{-5}	4×10^{-3}, 6×10^{-3}	0.007 ± 0.002[b]
Rigel.....	3×10^{-2}	6×10^{-2}	7×10^{-3}, 7×10^{-2}	2×10^{-5}, 9×10^{-4}	9×10^{-2}, 2×10^{-1}	0.1960 ± 0.0096
Vega.....	2×10^{-2}	3×10^{-2}	4×10^{-3}, 4×10^{-2}	2×10^{-5}, 1×10^{-3}	6×10^{-2}, 9×10^{-2}	0.0937 ± 0.0035
β Aur.....	2×10^{-3}	3×10^{-3}	5×10^{-4}, 5×10^{-3}	3×10^{-6}, 2×10^{-4}	6×10^{-3}, 1×10^{-2}	0.0078 ± 0.0019
β Car	3×10^{-3}	5×10^{-3}	6×10^{-4}, 6×10^{-3}	4×10^{-6}, 2×10^{-4}	8×10^{-3}, 1×10^{-2}	0.0111 ± 0.0010
GJ 124	1×10^{-7}	3×10^{-5}	3×10^{-6}, 6×10^{-5}	3×10^{-7}, 1×10^{-5}	3×10^{-5}, 1×10^{-4}	$< 1 \times 10^{-3}$[b]
GJ 139	6×10^{-8}	7×10^{-6}	1×10^{-6}, 6×10^{-5}	2×10^{-7}, 6×10^{-6}	8×10^{-6}, 7×10^{-5}	$< 1 \times 10^{-3}$[b]
Betelgeuse.....	4×10^{-7}	5×10^{-6}	1×10^{-6}, 7×10^{-5}	3×10^{-6}, 6×10^{-5}	1×10^{-5}, 1×10^{-4}	<0.0005

[a] The two values quoted for the estimated count rate at wavelengths longer than 2500 Å are derived with the two HRI different effective-area models in Paper I.

[b] The measured PSPC rate has been converted into the expected X-ray HRI rate using the PIMMS software and adopting a single temperature Raymond-Smith (RS) model. This rate has been subtracted from the measured HRI rate to derive the UV/visible contamination rate. The adopted parameters for the RS model are, namely, HD 46150 ($kT = 0.86$ keV, $N_H = 2.2 \times 10^{21}$), ζ Ori ($kT = 0.22$ keV, $N_H = 3.0 \times 10^{20}$), γ Cas ($kT = 0.86$ keV, $N_H = 2.0 \times 10^{20}$), Alcyone ($kT = 0.86$ keV, $N_H = 2.0 \times 10^{20}$), Hz-2168 ($kT = 0.86$ keV, $N_H = 2.0 \times 10^{20}$), GJ 124 ($kT = 0.86$ keV, $N_H = 1.0 \times 10^{18}$), and GJ 139 ($kT = 0.86$ keV, $N_H = 1.0 \times 10^{18}$).

area models given in Paper I, and, therefore, we cannot put new constraints on our knowledge of the *ROSAT* HRI UV/visible sensitivity. The same argument is valid for the two nearby G type stars (GJ 124, GJ 139) where the estimated UV/visible contamination is very low and consistent with the measured rate.

Our estimate of the HRI count rate for Betelgeuse is only within a factor of 2–3, with respect to the new estimate given by Berghöfer et al. (2000). The small difference between our estimate and the one in Berghöfer et al. (2000) is likely due to the fact that they use a Kurucz synthetic spectrum for Betelgeuse, while we use a measured, calibrated spectrum of a parent spectral-type star.

The comparison between HRI in-flight measurements and predicted UV/visible contamination rates, here presented for a few sample stars, confirm that the HRI UV/visible effective-area model provided in Paper I is fully representative of the in-flight performance of the instrument.

In the next section we use the model provided in Paper I to establish for which spectral-type stars it is important to account for possible UV/visible contamination in the *ROSAT* HRI observations and to quantitatively estimate the amount of this contamination.

3. THE HRI UV/VISIBLE CONTAMINATION FOR STELLAR SOURCES

In order to provide useful calibration curves to estimate the HRI UV/visible count rates from stars of different spectral types, we have selected a set of stars, covering the entire range of $T_{\rm eff} = 3000$–40,000 K, where a low-dispersion, *IUE*-calibrated spectrum was available. Notice that the choice of these stars is nearly arbitrary and is driven by the attempt to provide a good coverage of the above mentioned $T_{\rm eff}$ range.

Table 3 lists some relevant information about this new set of stars, including the reference number of the adopted *IUE* low-dispersion calibrated spectra.

The dereddened visible spectra (3500–7400 Å) for these stars were derived from calibrated spectra of parent spectral-type stars in Jacoby et al. (1984). The *IUE* spectrum of each one of these stars was dereddened, according to Seaton (1979), using the appropriate hydrogen column density (see Table 3). The dereddened UV/visible spectra of the sample stars were then normalized to $m_v = 0$ and attenuated by a given interstellar hydrogen column density N_H, ranging from 1×10^{19} cm^{-2} (nearly unabsorbed) to 5×10^{21} cm^{-2}. Figure 2 shows the dereddened UV/visible spectrum of one of the sample stars (*top curve*) and an example of how the absorption of an interstellar hydrogen column density of 2×10^{21} cm^{-2} affects the UV/visible stellar spectra.

The UV/visible spectra of the sample stars, normalized to $m_v = 0$, have been folded with the UV/visible HRI effective-area model, provided in Paper I. Figure 3 shows the curves of estimated HRI rate (1200–5500 Å) as a function of $T_{\rm eff}$ and hydrogen column density for stars of $m_v = 0$. At wavelengths longer than 2500 Å, we have used the estimated HRI rate derived with the higher effective-area model in Paper I (logarithmic interpolation). These curves can be used to estimate the UV/visible contamination rate in the *ROSAT* HRI observations of any star with known m_v, $T_{\rm eff}$, and N_H.

The linear regression plot of HRI count rate versus U magnitude given in Figure 2 of Berghöfer et al. (1999) represents one single point in our plot corresponding to $T_{\rm eff} \approx$ 10,000 K and $N_H \approx 1 \times 10^{19}$ cm^{-2}. Applying their plot to other spectral-type stars (e.g., a B0 star with $T_{\rm eff}$ about 30,000 K) or to higher hydrogen column density (e.g., $N_H \geq 2 \times 10^{21}$ cm^{-2}) may introduce an error of more than a factor of 10 in the estimate of the HRI UV/visible contamination count rates. The correlations provided in Figures 1 and 2 of Berghöfer et al. (1999) are, therefore, only valid for stars in the narrow spectral type range B8–A2 and low interstellar absorption ($N_H < 10^{20}$ cm^{-2}).

Figure 4 is a plot of the ratio of UV/visible (1200–5000 Å) to X-ray (0.1–2.4 keV) count rates for unabsorbed main-sequence stars. The adopted dereddened HRI UV/visible count rates have been previously described, while the

TABLE 3

LIST OF SAMPLE STARS COVERING THE T_{eff} RANGE 3000–40,000 K

Star	HR	HD	Spectral Type	V (mag)	T_{eff} (K)	$\log(N_H)$ (cm^{-2})	*IUE* Spectra
	8023	199579	O6 V	5.96	40,000	21.04	SWP 09429, LWP 03855
υ Ori.....	1855	36512	B0 V	4.62	30,000	20.35	SWP 08164, LWR 07097
λ Lib	5902	142096	B2.5 V	5.03	20,000	21.09	SWP 42326, LWR 10778
35 Eri	1244	25340	B5 V	5.28	15,000	20.06	SWP 49909, LWP 27312
Vega	7001	172167	A0 V	0.03	9500	18.00	SWP 27024, LWP 07904
70 Tau	1391	27991	F7 V	6.46	6500	19.00	SWP 09853, LWR 06639
V911 Tau	...	28099	G6 V	8.12	5500	19.00	SWP 09873, LWP 02601
Betelgeuse.....	2061	39801	M1 I	0.50	3200	19.80	SWP 37517, LWP 19982

adopted unabsorbed HRI X-ray count rates have been derived from the available *ROSAT* PSPC archival data of the sample stars, converted into an HRI X-ray rate using the PIMMS software. For this conversion we have adopted a single temperature RS model with $kT = 0.86$ keV and the interstellar absorption of each individual star given in Table 3.

For each spectral-type star we have assumed a range of X-ray luminosity based on the literature and listed in Table 4.

We notice that the UV/visible contamination for late-type stars (F–M types) is always negligible. For A-type stars, so far not known to be X-ray emitters, the HRI mea-

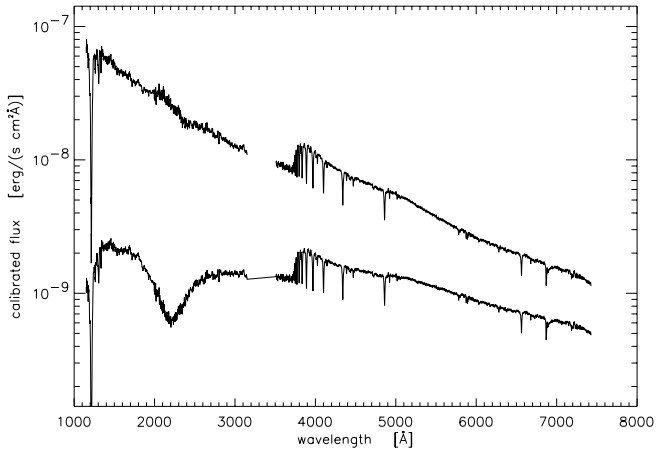

FIG. 2.—UV/visible calibrated spectrum of the sample star HD 25340 (B5 V). The top curve is the dereddened spectrum, while the bottom curve is the same spectrum attenuated by an interstellar hydrogen column density of 2×10^{21} cm^{-2}.

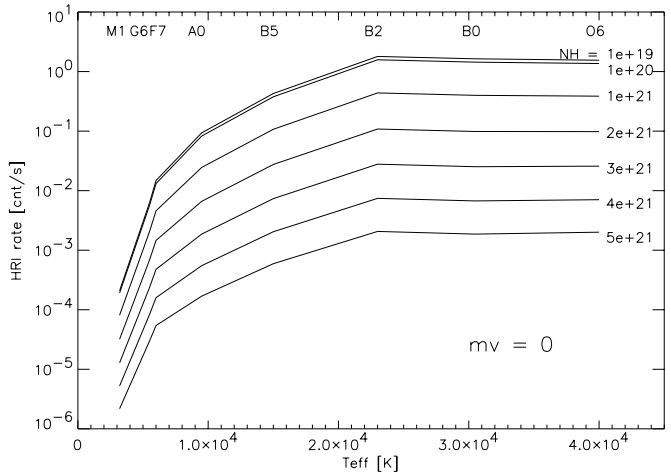

FIG. 3.—Estimated HRI rate (1200–5500 Å) for stars normalized to $m_v = 0$ as a function of T_{eff} and N_H.

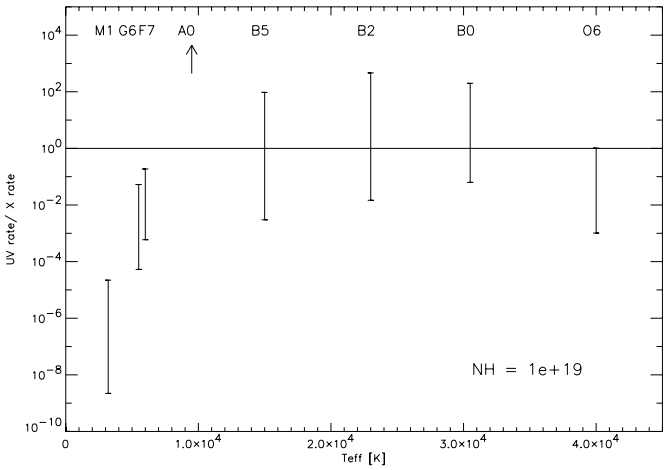

FIG. 4.—Ratio of the UV/visible (1200–5500 Å) to X-ray (0.1–2.4 keV) HRI rate for main-sequence stars as a function of T_{eff}. The bar on each data point takes into account the known range of X-ray activity for each spectral type.

TABLE 4

ADOPTED 0.1–2.4 keV X-RAY LUMINOSITY RANGE FOR MAIN-SEQUENCE STARS

Spectral Type	T_{eff} (K)	$\log(L_X)$ (ergs s^{-1})	Reference
O6 V	40,000	31.0–34.0	1
B0 V.....	30,000	29.0–32.5	1, 2
B2.5 V.....	20,000	27.5–32.0	1, 2
B5 V.....	15,000	27.5–32.0	1, 2
A0 V	9500	<25.5	3
F7 V.....	6500	27.0–29.5	3
G6 V	5500	26.5–29.5	3
M2 V.....	3200	25.5–29.5	4

REFERENCES.—(1) Berghöfer et al. 1997; (2) Cohen, Cassinelli, & MacFarlane 1997; (3) Schmitt 1997; (4) Schmitt et al. 1995.

surements can be considered entirely due to UV contamination. For early-type stars, the relevance of the UV contamination depends on the X-ray activity.

Figure 4 is a quick-look reference plot useful to understand for which spectral-type stars and which level of X-ray activity it is necessary to account for possible UV/visible contamination in an HRI observation. However, the usage of the curves in Figure 3 is recommended for a more quantitative estimate of the specific HRI UV/visible contamination for a given star with known m_v, $N_{\rm H}$, and $T_{\rm eff}$.

In order to estimate the HRI UV/visible contamination from other nonstandard stellar spectrum sources, we suggest to fold the UV/visible spectrum of the source with the HRI effective-area model we provided in Paper I.[5]

4. SUMMARY AND CONCLUSIONS

The *ROSAT* HRI UV/visible effective-area model presented in Paper I is based on laboratory measurements conducted within the *ROSAT* HRI ground calibration program. To provide an in-flight calibration of this model we have selected a set of stars observed with both the *ROSAT* PSPC and the HRI where the UV/visible calibrated spectrum was also available.

The comparison between measured and model-estimated UV/visible contamination rates for this set of stars confirms the validity of the ground calibration model in Paper I. These results also suggest that the actual HRI UV/visible effective area is likely closer to the high-sensitivity model (logarithmic interpolation) among the two provided in Paper I at wavelengths longer than 2500 Å.

[5] Available in tabular format at the Web page http://hea-www.harvard.edu/HRC/rosat/uvqe.txt.

The count rates estimated with the two models for Betelgeuse, a late-type giant with a cool photosphere and also negligible X-ray emission, are both in agreement with the measured HRI upper limit. Our estimate of the HRI count rate for Betelgeuse is only within a factor of 2–3 with respect to the new estimate given by Berghöfer et al. (2000) in an erratum recently published to revise their previous estimate (Berghöfer et al. 1999) which was more than 2 orders of magnitude higher.

Since the UV/visible contamination on HRI observations is strongly dependent on the source spectrum and on the interstellar absorption, we have provided useful calibration curves to estimate the HRI UV/visible contamination count rates from any star of given $T_{\rm eff}$, m_v, and $N_{\rm H}$.

The UV/visible contamination for late-type stars in the spectral type range G–M is always negligible. For the F-type stars a small nonnegligible UV contamination may be present in the case of very faint X-ray sources ($L_{\rm X} < 10^{27}$ergs s^{-1}). For A-type stars, HRI count rates can be entirely attributed to UV contamination. For early-type stars the degree of UV/visible contamination depends on the X-ray activity and $N_{\rm H}$ and can be a very large fraction of the detected count rates, especially for B-type stars.

We acknowledge partial support by Agenzia Spaziale Italiana (M. B., A. C., G. M.), Ministero della Ricerca Scientifica e Tecnologica (M. B., A. C., G. M.), and NASA contract NA8-38248 (M. V. Z., S. S. M.). We acknowledge usage of the *IUE* Final Archive maintained by the European Space Agency at VILSPA, the SIMBAD astronomical database of the Centre de Donnée Astronomiques de Strasbourg, and the *ROSAT* data archive of the Max Planck Institut für extraterrestrische Physik.

REFERENCES

Barbera, M., Collura, A., Dara, A., Leone, M., Powell, F. R., Serio, S., Varisco, S., & Zombeck, M. V. 1997, Exp. Astron., 7, 51
Berghöfer, T. W., Schmitt, J. H. M. M., & Cassinelli, J. P. 1996, A&AS, 118, 481
Berghöfer, T. W., Schmitt, J. H. M. M., Danner, R., & Cassinelli, J. P. 1997, A&A, 322, 167
Berghöfer, T. W., Schmitt, J. H. M. M., & Hünsch, M. 1999, A&A, 342, L17
Berghöfer, T. W., Schmitt, J. H. M. M., & Hünsch, M. 2000, A&A, 357, 387
Cohen, D. H., Cassinelli, J. P., & MacFarlane, J. J. 1997, ApJ, 487, 867
Damiani, F., Maggio, A., Micela, G., & Sciortino, S. 1997, ApJ, 483, 350
David, L. P., Harden, F. R., Jr., Kearns, K. E., & Zombeck, M. V. 1995, The *ROSAT* High Resolution Imager (Cambridge: *ROSAT* Science Data Center)
Jacoby, G. H., Hunter, D. A., & Christian, C. A. 1984, ApJS, 56, 257
Micela, G., et al. 1999, A&A, 341, 751
Micela, G., Sciortino, S., Kashyap, V., Harden, F. R., Jr., & Rosner, R. 1996, ApJS, 102, 75
Murray, et al. 1997, Proc. SPIE, 3114, 11
Schmitt, J. H. M. M. 1997, A&A, 318, 215
Schmitt, J. H. M. M., Fleming, T. A., & Giampapa, M. S. 1995, ApJ, 450, 392
Schmitt, J. H. M. M., Golub, L., Harnden, F. R., Jr., Maxson, C. W., Rosner, R., & Vaiana, G. S. 1985, ApJ, 290, 307
Seaton, M. J. 1979, MNRAS, 187, 73P
Zombeck, M. V., Barbera, M., Collura, A., & Murray, S. S. 1997, ApJ, 487, L69 (Paper I)